Journal of Solid State Chemistry **148,** 143–149 (1999)
Article ID jssc.1999.8407, available online at http://www.idealibrary.com on IDEAL®

Electronic Structure of Vacancy Ordered Spinels, $GaMo_4S_8$ and GaV_4S_8, from *ab Initio* Calculations

N. Shanthi and D. D. Sarma[1]

Solid State and Structural Chemistry Unit, Indian Institute of Science, Bangalore 560012, India

Received February 16, 1999; in revised form May 13, 1999; accepted May 28, 1999

THIS WORK IS DEDICATED TO PROF. C. N. R. RAO FOR THE SPECIAL FESTSCHRIFT VOLUME ON THE OCCASION OF HIS 65TH BIRTHDAY

We report *ab initio* calculations for the band dispersions and total as well as partial densities of states for vacancy ordered, clustered spinels, $GaMo_4S_8$ and GaV_4S_8. Results are presented for the high temperature cubic phase for both compounds. Additionally, we discuss results of similar calculations for $GaMo_4S_8$ in an idealized cubic structure, as well as the nonmagnetic and the ferromagnetic states of the low temperature rhombohedral structure. Comparison of these results allows us to discuss the unusual aspects of the electronic structure of this interesting class of compounds, and provide estimates of the crystal-field and exchange splitting strengths.

Key Words: **electronic band structure; vacancy ordered spinel; linearized muffin-tin orbital method.**

INTRODUCTION

Compounds with the general formula AB_2X_4 form in the well-known structural type called spinels (1). In this structure, A cations occupy the tetrahedral sites with the B cations in the octahedral sites formed by anions, X, arranged in a cubic close-packed lattice. An interesting variation of this structural motif is provided by compounds AB_4X_8 such as $GaMo_4S_8$ (2, 3) and GaV_4S_8 (4). In the case of these cation-deficient spinels, only half of the tetrahedral sites are occupied by the A cation, leaving the other sites vacant. When the A cation is a trivalent ion, such as Ga^{3+} or Al^{3+}, it is found that the A cations and vacancies order (5) themselves among the tetrahedral sites in the ratio 1:1. This leads to the reduction in the symmetry of the cubic $Fd3m$ group to the $F\bar{4}3m$. The vacancies in the tetrahedral sites allow the B cations to come closer together, forming metallic tetrahedral clusters involving four B cations, with typical intra cluster B–B distances of 2.8 Å and intercluster distances of more than 4 Å. Such a clustering of B atoms leads to strong intracluster metallic bonding, though the intercluster interaction is expected to be weak. It is known that compounds with Mo_6 octahedral clusters (chevrel phases) exhibit high-critical field superconductivity; in contrast Mo_4 clusters are prone to ferromagnetic instabilities at low temperatures. Additionally, the overall charge neutrality requires unusual oxidation states at the B sites. These facts lead to interesting electronic and magnetic properties for this class of compounds. Thus, it has been found that compounds belonging to this structure-type exhibit different magnetic properties; for example, $Mo_4S_4I_4$ is diamagnetic, $GaNb_4X_8$ and $GaTa_4X_8$ are paramagnetic, and $GaMo_4S_8$ is ferromagnetic. Moreover, fractional occupancies at the transition metal sites arising from the unusual oxidation states should be expected to give rise to a metallic behavior, while in reality most of these exhibit semiconducting behavior. This would indicate a strong electron–electron correlation effect, though the Coulomb interaction strength within the Mo 4d states is not expected to be as large as in the case of 3d transition metal ions.

Specifically, in the case of $GaMo_4S_8$, there is a structural transition from the high temperature cubic phase to a rhombohedral phase, with $T_{tr} = 46.5$ K. $GaMo_4S_8$ is found to be weakly ferromagnetic (1) below a T_c of 13 K. The magnetic moment per cluster has been reported to be 1.84 μ_B (5) and 1 μ_B (6). GaV_4S_8 shows a structural phase transition around 46 K. GaV_4S_8 is shown (7) to behave like a Fermi-glass, due to the large intercluster distances of MoS_6 octahedra.

There have been a lot of studies of the electrical and magnetic properties of these spinels and also of the specific heat and Seeback coefficients. Comparitively, there are few electronic structure investigations of this class of compounds (8, 9). One earlier study (8) calculated the band structure of GaM_4X_8-type compounds within the extended Hückel tight binding calculations. It was found that the metal–metal interaction in such clustered compounds is

[1] To whom correpondence should be addressed. Fax: 91-80-3311310. E-mail: sarma@sscu.iisc.ernet.in. Also at the Jawaharlal Nehru Centre for Advanced Scientific Research, Bangalore.

0022-4596/99 $30.00

strongly modified by the presence of the ligand atoms. In the present investigation, we report *ab initio* band structure calculations and discuss the details of the electronic structure in various crystallographic modifications of $GaMo_4S_8$ and also in GaV_4S_8. To date, the only *ab initio* band structure investigation for any compound in this class has been carried out for GeV_4X_8 ($X = S, Se$) (9). The DOS of GeV_4S_8 (9) is similar to the DOS of GaV_4S_8 reported in the present work. Here, we report a detailed electronic band structure investigation of $GaMo_4S_8$ and GaV_4S_8, in terms of total and partial densities of states, as well as band dispersions.

METHOD OF CALCULATION

Band structure calculations within the local density approximation were performed using the linearized muffin-tin orbital (LMTO) method, in the atomic sphere approximation (ASA) (10). In the case of ASA, a sphere is inscribed around each atom, with the radii of the spheres chosen in such a way that the sum of the volumes of the spheres equals the volume of the unit cell. The potential within each sphere is assumed to be spherically symmetric, with a constant potential in the intersphere region. In close-packed structures, it is possible to construct such spheres around each atom without very strong overlaps between different spheres. However, in compounds such as the ones being investigated here, the use of only atomic spheres with the volume-filling criterion leads to unphysically large ($\sim 35\%$) radial overlaps. In such open structures the volume-filling criterion is met by additional introduction of "empty spheres" that are not centered on atomic sites. This helps in achieving a better description of the potential and leads to more accurate results. In the present cases, we include 15 empty spheres along with the 13 atomic spheres to achieve the volume-filling criterion with modest ($\leq 18\%$) radial overlaps. In each sphere, *s*, *p*, and *d* orbitals were used as basis. The sphere radii used were 2.24 a.u. for Ga, 2.5 a.u. for Mo, 2.88 a.u. for S, and 2.4 a.u. for V; the radii of empty spheres were in the range 1.45–2.3 a.u., depending on the position and the compound.

Both GaV_4S_8 and $GaMo_4S_8$ form as cubic spinels with space group $F\bar{4}3m$, with the lattice constants $a = 9.68$ and 9.7356 Å (2), respectively. In the low temperature phase, the structures belong to the $R3m$ space group ($a_{rh} = 6.8506$ Å and $\alpha_{rh} = 60.533$ Å for $GaMo_4S_8$). In the low temperature distorted phase, $GaMo_4S_8$ also shows weak ferromagnetism. We have carried out self-consistent calculations in the case of $GaMo_4S_8$ for both crystal structures and in the case of GaV_4S_8 for the cubic crystal structure. In the case of $GaMo_4S_8$, an additional spin-polarized scalar relativistic calculation was carried out for the ferromagnetic structure. In all these calculations, self-consistency was achieved with 216 ($6 \times 6 \times 6$) **k** points in the Brillouin zone. This corresponds to 18, 18, and 68 **k** points in the irreducible part of the Brillouin zone for ideal cubic, cubic, and rhombohedral structures, respectively.

In order to understand the complicated spinel structure better, we have also performed calculations for the idealized-cubic spinel structure. This enables us to establish the role of distortion of Mo–S or V–S octahedra in the real structure and also that of clustering of Mo or V atoms, that are reportedly responsible for the various magnetic behaviors of these spinel compounds. In this case also, we have used *s*, *p*, and *d* as basis and obtained self-consistent band structures with 216 **k** points in the Brillouin zone (18 **k** in the irreducible part).

RESULTS AND DISCUSSION

The real crystal structure of compounds with the general formula MM'_4X_8, with M = Ga, Al, etc., M' = Cr, V, Mo, etc., and X = S or Se, is complicated both in the high and low temperature modifications. They contain not only distortions in the near neighbor coordination of $M'X_6$ octahedra but also M' clustering involving four atoms. In these M'_4 clusters the M'–M' distances are often comparable to those of the elemental metal. Therefore, the electronic structure of these compounds is not only governed by the nearest neighbor transition metal (M') *d*-ligand (X) *p* interactions, as in most other inorganic compounds of transition metals, but is also strongly influenced by M'–M' *d*–*d* interactions. These two (*d*–*d* and *d*–*p*) interactions compete with each other leading to interesting properties. In order to understand the effects of these two interactions separately, it is instructive to study these compounds in their idealized cubic structure, which is related to the real structure. In the case of the idealized cubic spinel structure of $GaMo_4S_8$, Mo atoms are surrounded by six sulphur ions to form regular octahedra of MoS_6 with Mo–S distances of 2.434 Å each. On the other hand, the nearest-neighbor Mo–Mo distances are 3.443 Å, which is significantly more than the corresponding Mo–Mo distances in the molybdenum metal (2.72 Å). This suppresses the Mo–Mo *d*–*d* interactions, and the electronic structure is expected to be dominated by the local Mo *d*–S *p* interactions within the MoS_6 octahedra. The fivefold degenerate Mo 4*d* levels split into triply degenerate t_{2g} and doubly degenerate e_g levels in the presence of the octahedral crystal field; the t_{2g} group of orbitals consists of d_{xy}, d_{yz}, and d_{zx} orbitals, while the e_g group consists of the $d_{x^2-y^2}$ and $d_{3z^2-r^2}$ Mo atomic orbitals. This splitting between t_{2g} and e_g is expected to be further enhanced by the anisotropic interactions between the Mo *d* and S *p* levels. The t_{2g} levels of Mo interact with the S *p* levels via $pd\pi$ interactions forming a bonding (t_{2g})–antibonding (t^*_{2g}) pair, while the Mo e_g levels interact with the S *p* levels through $pd\sigma$ hopping interactions, forming the bonding (e_g)–antibonding (e^*_g) levels. Since the $pd\sigma$ interaction is approximately twice as large as the $pd\pi$ one, the e_g–e^*_g splitting is

larger than the t_{2g}–t_{2g}^* splitting, enhancing the effective crystal field splitting, as mentioned before. These local cluster orbitals corresponding to t_{2g}, t_{2g}^*, e_g, and e_g^* are expected to mix between different clusters via the Mo–S–Mo hoppings, leading to the formation of the corresponding bands in the periodic solid. Due to the bare energy differences, we expect the antibonding (t_{2g}^* and e_g^*) bands to be mainly contributed by the transition metal d states, while the corresponding bonding bands will be dominated by the ligand p states. In order to discuss these effects in detail, we show the calculated nonmagnetic LMTO-ASA band dispersions along four symmetry directions in Fig. 1a, with the corresponding density of states (DOS) in Fig. 1b for $GaMo_4S_8$ in the idealized cubic structure. Since there are four atoms of Mo in each unit cell, we expect a total of 20 spin-degenerate d bands arising from Mo. Out of these, 12 will constitute the primarily t_{2g}^* band, the remaining 8 making the e_g^* band. Bands with -1.4, -1.1, -0.8, 0.5, and 0.8 eV energies at the Γ point have degeneracies of 1, 2, 3, 3, and 3, respectively making a total of 12 spin-degenerate t_{2g}^* bands which can be most easily observed along the X–Γ direction. The dispersion of these 12 t_{2g}^* bands along the various symmetry directions (Γ–L, L–W, W–X, and X–Γ) are rather small (<0.7 eV), particularly for those with higher energies (dispersional widths <0.2 eV), leading to relatively flat bands. These flat bands give rise to strongly structured DOS with sharp peaks in the energy range between -1.8 and 1 eV, as can be seen in Fig. 1b. In Fig. 1b, we have also shown the partial Mo d and S p partial densities of states along with the total DOS. A comparison of the partial DOS with the total makes it evident that the density of states over this energy range is dominated by the Mo d states with finite admixture of S p states. In a similar way, one can observe eight bands between 2.1 and 4.1 eV in Fig. 1a. These eight spin-degenerate e_g^* bands are most easily seen along the W–X direction, where all the degeneracies are lifted. These bands exhibit enhanced dispersion compared to the t_{2g}^* bands. The corresponding DOS appearing in the unoccupied part, above E_F, extends between 1 and 4 eV with dominant Mo d character, as can be observed from the partial DOS (Fig. 1b). It can be noticed that though Mo d contribution is dominant for both t_{2g}^* and e_g^* bands, the relative contribution from S p states is considerably larger in the energy region of the e_g^* band compared to that in the t_{2g}^* region. This enhanced admixture of S p states arises from the fact that the $pd\sigma$ interaction responsible for the e_g^* states is considerably larger than the $pd\pi$ interactions giving rise to the t_{2g}^* states. From Fig. 1b, we find that the effective crystal-field splitting measured from the centroids of the t_{2g}^* and e_g^* is about 2.6 eV. This splitting leads to the formation of a very small gap between the t_{2g}^* and e_g^* bands, as shown in Fig. 1b. The remaining 24 bands arise from the three p-orbitals on each of the eight sulphur ions and can be observed in the energy range between -8 and -1.8 eV.

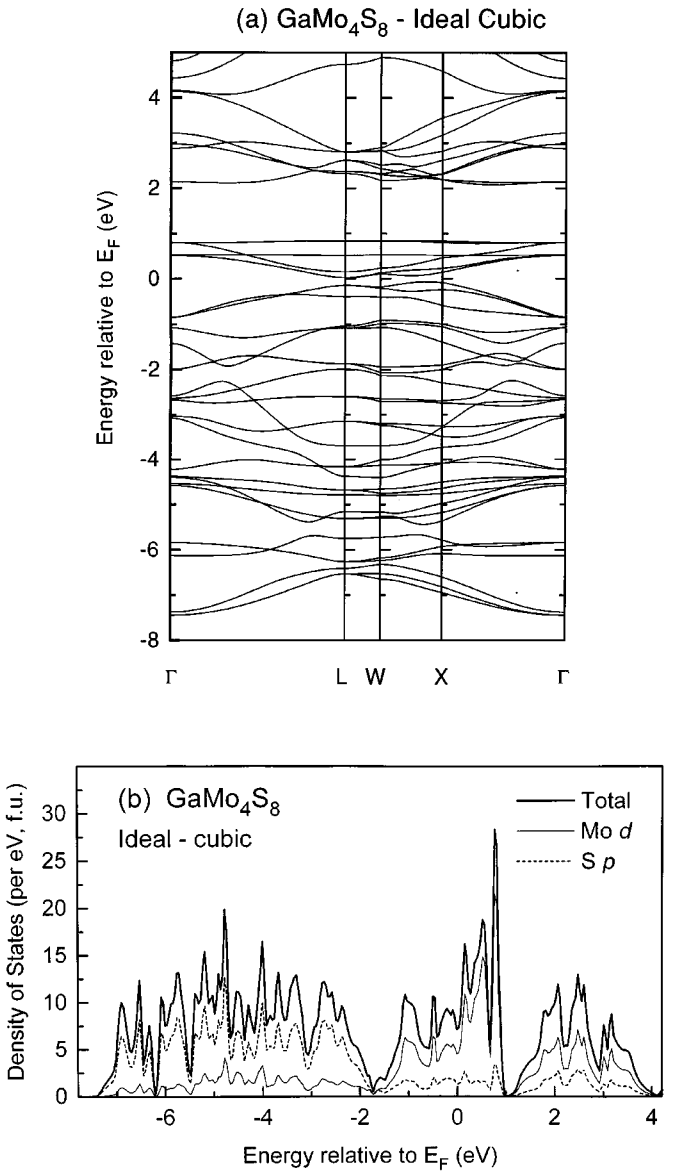

FIG. 1. (a) Band dispersions along the various symmetry directions in the case of nonmagnetic $GaMo_4S_8$ in the idealized cubic structure. (b) The total (thick line), partial Mo d (thin line), and partial S p (dashed line) densities of states corresponding to the band dispersions shown in panel (a).

The total and partial densities of states in Fig. 1b show that this region is dominated by S p states with finite Mo d admixture. These correspond to overlapping t_{2g} and e_g bands that are the bonding counterparts of the antibonding t_{2g}^* and e_g^* bands. From the DOS shown in Fig. 1b, it can be seen that the total DOS is almost entirely made up of Mo d and S p states, suggesting that the electronic structure in the ideal case is dominated by the local Mo d–S p interactions. Having understood the electronic structure of the idealized cubic $GaMo_4S_8$ in terms of the Mo d–S p interactions, we now turn to the real crystal structures in order to investigate

the effects of transition metal clustering on the electronic structures of these compounds.

In the high temperature nonmagnetic phase, the real crystal structure of $GaMo_4S_8$ corresponds to the space group $F\bar{4}3m$. Although it forms in the cubic space group, the structure is already a distorted one from the idealized cubic spinel structure discussed above. In this structure, Mo atoms are displaced toward the vacancies at the tetrahedral sites, forming tetrahedral clusters of Mo atoms. Intracluster Mo–Mo distances are 2.814 Å, comparable to the Mo–Mo distances in the elemental molybdenum metal, as pointed out earlier. The intercluster distances are much larger (4.07 Å). Thus, one expects the intracluster Mo–Mo *d*–*d* interactions to play a more dominant role in the real structure compared to that in the case of the idealized one and to compete with the Mo *d*–S *p* interactions. Moreover, MoS_6 octahedra are no more regular, but distorted, with three sulphur ions at 2.345 Å and three others at 2.602 Å, respectively. Such distortions are expected to lift the degeneracies of various bands at the symmetry points. Figure 2a shows the LMTO-ASA band dispersions for $GaMo_4S_8$ in the real cubic spinel structure, and Fig. 2b shows the corresponding total density of states along with the Mo *d* and S *p* partial densities of states. In this case also, we find that the total density of states (Fig. 2b) over the entire energy region of interest is almost entirely composed of Mo *d* and S *p* states. However, both band dispersions and the DOS are considerably different in this case compared to those in the ideal cubic structure (Fig. 1). Thus, we find that two triply degenerate bands originate at the Γ point with energies -1.0 and -0.2 eV (Fig. 2a). Moreover, these two groups of bands are clearly separated from each other with a finite gap along all the symmetry directions. Furthermore, there are altogether fourteen bands clearly separated from the lower six bands by a large energy gap, dispersing in the energy interval between 1.7 and 4.8 eV. In the case of the ideal cubic structure, the lower energy group of twelve bands associated with t_{2g}^* bands arises basically from the Mo *d*–S *p* $pd\pi$ interactions within the MoS_6 octahedral clusters. While the finite distortion of the MoS_6 cluster from the octahedral geometry in the real structure is expected to lift the degeneracy of the t_{2g}^* bands, it cannot be responsible for such strong changes in the dispersions, where only six of the twelve bands are observed in the relevant energy range of the t_{2g}^* bands. Thus, it is clear that Mo *d*–*d* interaction within the local Mo_4 cluster leads to significant changes in the electronic structure of this compound. In particular, the twelve t_{2g}^* levels arising from 4 Mo atoms interact with each other due to Mo clustering and further subdivide into bonding and antibonding levels, each containing six states. This *d*–*d* interaction involving the t_{2g} levels is particularly strong due to the tetrahedral geometry of the four Mo atoms and the short Mo–Mo bond lengths; thus, the antibonding six levels are pushed up into the originally e_g^* group of levels

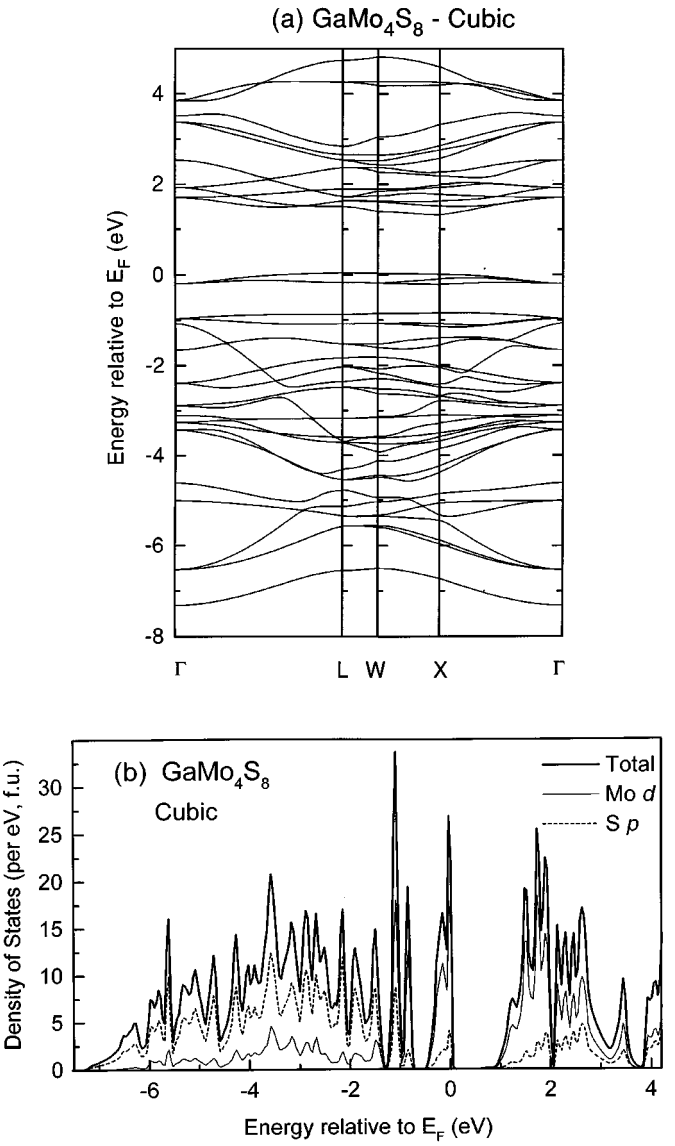

FIG. 2. (a) Band dispersions along the various symmetry directions in the case of nonmagnetic $GaMo_4S_8$ in the real cubic structure. (b) The total (thick line), partial Mo *d* (thin line), and partial S *p* (dashed line) densities of states corresponding to the band dispersions shown in panel (a).

lying between 2.1 and 4.1 eV. Of the six bonding levels with respect to Mo *d*–*d* interactions, the triply degenerate band at the Γ point just below E_F, at -0.2 eV, shows little dispersion due to the weak intercluster interaction and thus gives rise to a peaked DOS feature at E_F, well separated from other features. The other triply degenerate band at the Γ point at -1.0 eV, giving rise to a two-peak DOS structure, overlaps the top of primarily S *p* derived states, as can be clearly seen in Fig. 2b. For these states also, Mo *d* contribution is dominant, though sulphur *p* contribution increases significantly, particularly for the lower energy DOS

feature at -1.2 eV. In the energy region of e_g^* bands of the ideal cubic case (Fig. 1), now there are 14 bands between about 1.7 and 4.8 eV. These are separated from the bands near E_F by 1.5 eV. Thus, it can be seen that the Mo–Mo d–d interactions play a dominant role, opening up a much larger gap between the subgroups of d-bands compared to that arising from the crystal field effects in the case of ideal spinels without any clustering of the transition metal ions.

The low temperature modification of $GaMo_4S_8$ is a rhombohedral structure in the space group $R3m$. In this space group, the distortions make the Mo sites inequivalent, and there are two types of Mo atoms (Mo1 and Mo2). In each unit cell, there is one Mo1 and three Mo2 atoms, unlike in the case of the cubic high temperature structure. However, in the low temperature phase also, there is a clustering of Mo atoms and the MoS_6 octahedra are distorted as in the case of real cubic high temperature structure. The intracluster and intercluster Mo–Mo distances are not very different from the real cubic case, being 2.823 Å and 4.028 Å, respectively. Also, the Mo atom has three sulfurs at distance 2.414 Å and three more sulphur atoms at 2.576 Å, respectively. Thus, the MoS_6 octahedra are slightly less distorted compared to the real cubic case. Therefore, the band dispersions and the density of states cannot be very different from the real cubic high temperature structure. The density of states shown in Fig. 3b indeed confirms this, as it is seen to be quite similar to the real cubic spinel structure shown in Fig. 2b. In Fig. 3a, we show the band dispersions along Γ–L and Γ–Z directions for the $GaMo_4S_8$ rhombohedral structure. From the band dispersions it can be seen that the distortions in the rhombohedral structure lift some of the degeneracies of the bands at the Γ point by small energies. For example, the triply degenerate band closest to E_F in the real cubic case has now split into two bands, a singly degenerate one and a doubly degenerate one. Similarly, in the unoccupied part between 1.7 and 4.8 eV, all the triply degerate bands split into singly and doubly degenerate bands. In Fig. 3b, we also show the partial densities of states for the Mo1 d, Mo2 d, and S p states. It is seen that the partial DOS from Mo2 is approximately thrice that of Mo1, as there are three Mo2 atoms and one Mo1 atom in the unit cell.

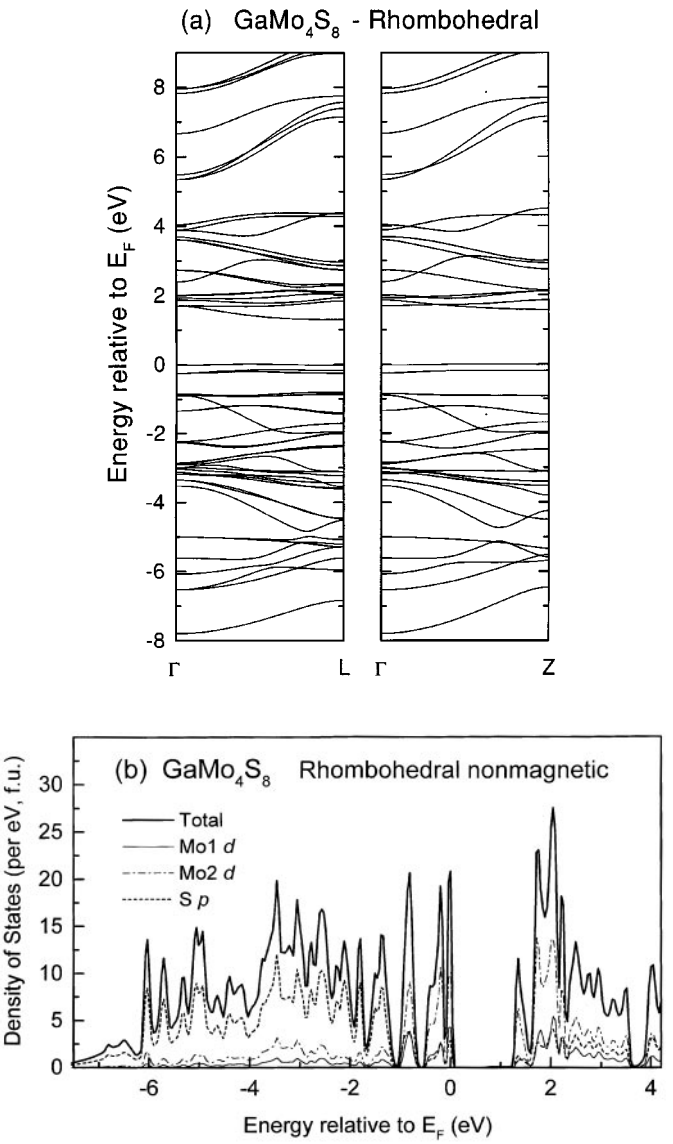

FIG. 3. (a) Band dispersions along the various symmetry directions in the case of nonmagnetic $GaMo_4S_8$ in the low temperature rhombohedral structure. (b) The total (thick line), partial Mo1 d (thin line), partial Mo2 d (dash-dotted line), and partial S p (dashed line) densities of states corresponding to the band dispersions shown in panel (a).

$GaMo_4S_8$ is weakly ferromagnetic below a temperature of 19.5 K. In order to understand the magnetic structure, we have carried out the spin-polarized calculations within the scalar-realistivistic version of LMTO-ASA. In Fig. 4a, we show the total and partial densities of states arising from total Mo d and S p contributions for $GaMo_4S_8$. The total DOS in this case is not very different compared to the nonmagnetic calculation shown in Fig. 3. This suggests a weakly magnetic state with a small exchange splitting compared to the dispersional widths of various bands. In the reverse scenario of an exchange splitting substantially larger than the band widths, we would expect to see new features in DOS arising from the exchange splittings in the magnetic state in comparison to the nonmagnetic state. Instead, we only see a small decrease in the energy gaps between the various subgroups of features in the DOS arising from primarily Mo d states. In Fig. 4b, the up-spin and down-spin contributions from Mo1 d states to the DOS are shown separately, with the corresponding Mo2 d up and down partial densities of states being shown in Fig. 4c. The up- and down-spin partial DOS in each case (Fig. 4) are shifted with respect to each other by the intra-atomic

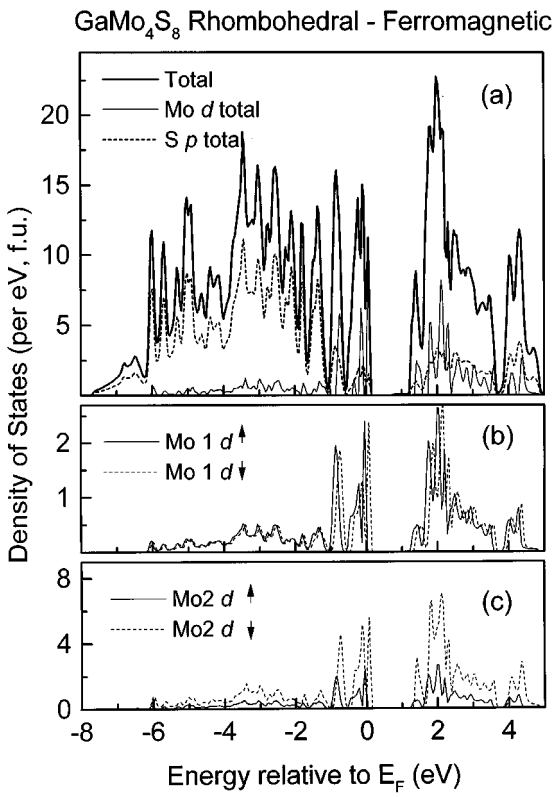

FIG. 4. Total and partial Mo *d* and S *p* densities of states for ferromagnetic $GaMo_4S_8$ in the low temperature rhombohedral structure. (a) Total (thick line), partial Mo *d* (thin line), and partial S *p* (dashed line) densities of states. (b) Mo1 *d* up-spin and down-spin partial densities of states. (c) Mo2 *d* up-spin and down-spin partial densities of states.

exchange splitting of less than ~ 0.2 eV. Consequently, there is a weak ferromagnetic moment associated with the Mo atoms. The calculated magnetic moment per cluster (i.e., four Mo atoms) is about 1 μ_B, which compares reasonably well with the experimental values 1 μ_B (6) and 1.84 μ_B (5) reported in the literature.

In order to understand whether the unusual electronic structure, as revealed by band structure calculations here, is typical of such vacancy ordered, clustered spinels, we have also carried out preliminary studies of the band structure of GaV_4S_8, which is a closely related compound to $GaMo_4S_8$. GaV_4S_8 also forms as a cubic spinel with the space group $F\bar{4}3m$ in the high temperature phase and goes through a structural transition around 45 K to the rhombohedral symmetry group of $R3m$ at low temperatures. We have carried out band structure calculations for the cubic crystal structure and report the various densities of states to point out the similarities between the two cases of GaV_4S_8 and $GaMo_4S_8$. In this case also, there is a clustering of vanadium atoms, with intracluster V–V distances of 3.168 Å and intercluster distances of 3.677 Å, respectively. Although, the intracluster distance is not as drastically short as in the case of $GaMo_4S_8$ (2.823 Å), it is still comparable to the V–V distances in the metallic vanadium of 3.028 Å. Thus, in this case also, the V–V *d*–*d* interaction is expected to dominate over the V *d*–S *p* interactions. Figure 5 shows the density of states of GaV_4S_8 in the high temperature $F\bar{4}3m$. The densities of states in this case are very similar to that of $GaMo_4S_8$ (Fig. 2b), and the various features are describable in terms of that for the corresponding DOS of $GaMo_4S_8$ in the real cubic structure. In Fig. 5, the V–V interactions within the V_4 cluster open up a gap (~ 0.2 eV) at about -0.3 eV. The gap between these and the e_g^*-like bands is about 0.7 eV, as compared to 1.5 eV in the case of $GaMo_4S_8$.

While it is clear that the particular type of transition metal clustering in these compounds dominates the electronic structure, the most unusual aspect evidently is the formation of a very narrow band (width ~ 0.7 eV) at the Fermi energy; clearly these states are responsible for the transport and magnetic properties. There are two distinct effects arising from the clustering in these compounds. In the first place, intracluster *d*–*d* interactions lead to significant redistribution of the *d* bands. Such an effect takes place in many compounds where significant clustering of the transition metals is observed. For example, in Mo_2S_3 (11), $CoMo_2S_4$ (12), and Mo_2As_3 (13), Mo ions form as zigzag chains; in MoN (14), it forms triangular clusters; in Mo_3Se_4 (15) and $PbMo_6S_8$ (16), it forms octahedral clusters; and in phosphides, it forms a more complicated but metallic network. It is also known that in the chevrel phases, it even gives rise to superconductivity. Only in the semiconducting spinels (such as $GaMo_4S_8$), is Mo found to support local magnetic moments, suggesting an enhanced effect of electron correlation. This is evidently due to the fact that the Mo_4 tetrahedra are isolated from each other with a large intercluster separation. This reduced intercluster coupling leads to very flat bands and a narrow band width (W) at the

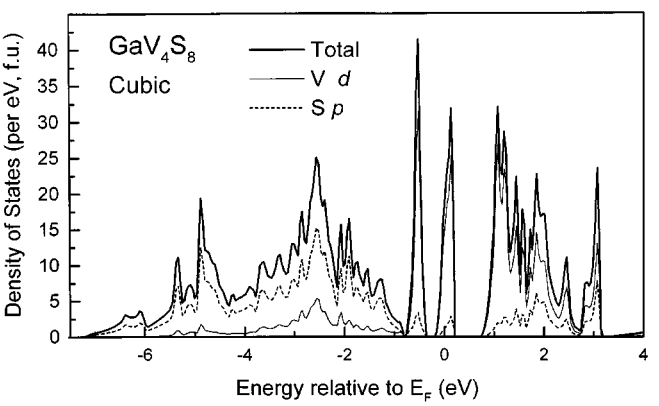

FIG. 5. The total and partial V *d* and S *p* densities of states for GaV_4S_8 in the high temperature cubic crystal structure.

Fermi energy. Thus, in spite of a modest Coulomb interaction strength (U) within the Mo 4d states, overall correlation effect, as measured by U/W, is strongly enhanced due to the formation of narrow bands. Such narrow bands, with large U/W and a high density of states at E_F, are indeed unstable with respect to magnetic ordering. We believe that the semiconducting behavior in these systems is helped by the formation of a Hubbard splitting of the band at E_F, forming an occupied lower Hubbard band and an unoccupied upper Hubbard band. A similar view has been also suggested (9) for the installing nature of GeV_4X_8 (X = S, Se). While an effective single particle calculation, such as LMTO, cannot describe the Hubbard splitting of correlated bands, the results presented here are strongly suggestive of such a mechanism. The splitting between the upper and the lower Hubbard bands is expected to be in the order of U. Thus, as long as U is larger than the relevant bandwidth ($\sim$0.7 eV), a gap (or at least a pseudo-gap) indeed is expected to open at the chemical potential. Such a modest value of U is not unreasonable even for the 4d states of Mo. It is also expected that disorder effects may further accentuate the semiconducting behavior, particularly in the presence of a pseudogap resulting in low DOS at E_F.

In conclusion, we have presented detailed band structure results for $GaMo_4S_8$ in the idealized cubic and real structures in order to elucidate the electronic structure of this compound. We have pointed out the relative importance of Mo d–S p and Mo d–Mo d competing interactions in this compound and related the unusual properties to these effects. We have also estimated crystal-field and exchange splittings. Preliminary results from a closely related compound, GaV_4S_8, are also discussed.

ACKNOWLEDGMENTS

The authors thank Dr. M. Methfessel, Dr. A.T. Paxton, and Dr. M. van Schiljgaarde for making the LMTO-ASA band structure program available. We thankfully acknowledge the use of computational facilities provided by the Supercomputer Education and Research Centre, Indian Institute of Science.

REFERENCES

1. A. R. West, "Solid State Chemistry and its Applications." Wiley, New York, 1984.
2. M. Francois, W. Lengauer, K. Yvon, H. Ben Yaich-Aerrache, P. Gougeon, M. Potel, and M. Sergent, *Z. Kristallographie* **196,** 111 (1991).
3. H. Barz, *Mater. Res. Bull.* **8,** 983 (1973).
4. D. Brasen, J. M. Vandenberg, M. Robbins, R. M. Willens, W. A. Reed, R. C. Sherwood, and X. J. Pinder, *J. Solid State Chem.* **13,** 298 (1975).
5. J. M. Vandenberg, and D. Brasen, *J. Solid State Chem.* **14,** 203 (1975).
6. A. K. Rastogi, A. Berton, J. Chaussy, R. Tournier, M. Potel, R. Chevrel, and M. Sergent, *J. Low Temp. Phys.* **52,** 539 (1983).
7. Y. Sahoo and A. K. Rastogi, *J. Phy. Condens. Matter* **5,** 5953 (1993).
8. A. Le Beuze, H. Loirat, M. C. Zerrouki, and R. Lissillour, *J. Solid State Chem.* **120,** 80 (1995).
9. D. Johrendt, *Z. Anorg. Allg. Chem.* **624,** 952 (1998).
10. O. K. Andersen, *Phys. Rev. B* **12,** 3060 (1975); O. K. Andersen and R. V. Kasowski, *Phys. Rev. B* **4,** 1064 (1971); O. K. Andersen, *Solid State Commun.* **13,** 133 (1973).
11. R. de Jonge, T. Popma, G. A. Wiegers, and F. Jellinek, *J. Solid State Chem.* **2,** 188 (1970).
12. J. M. Vandenberg, *Inorg. Chim. Acta* **2,** 216 (1968).
13. F. Hulliger, "Structure and Bonding," Vol. 4, p. 141. Springer-Verlag, New York, 1968.
14. J. M. Vandenberg and B. T. Matthias, *Mater Res. Bull.* **9,** 1085 (1974).
15. O. Bars, J. Guillevic, and D. Grandjean, *J. Solid State Chem.* **6,** 48 (1973).
16. M. Marezio, P. D. Dernier, J. P. Remeika, E. Corenzwit, and B. T. Matthias, *Mater. Res. Bull.* **8,** 657 (1973).